6th International Conference
on
Wind Turbine Noise
Glasgow 20-23 April 2015

Aeroacoustic Simulation of an Airfoil in Turbulent Inflow

Jonas E. Illg*, Thorsten Lutz*, Ewald Krämer*
*** Institute of Aerodynamics and Gas Dynamics, Universität Stuttgart, Pfaffenwaldring 21, 70569 Stuttgart, Germany**
E-mail: illg@iag.uni-stuttgart.de

Summary

An airfoil was simulated in turbulent inflow conditions using a high order numerical scheme and a hybrid RANS/LES method. The numerical methods applied for flow simulation and noise prediction are described. Both turbulent inflow noise and turbulent boundary layer trailing edge noise emissions are evaluated, including the impact of inflow turbulence on trailing edge noise. The results show that a large portion of the airfoil surface, exceeding the leading edge region, is involved in broadband noise emission due to inflow turbulence. Frequencies of turbulent inflow noise emitted directly at the leading edge are lower than the frequency range of noise emitted on the airfoil surface downstream the leading edge. The peak frequency of trailing edge noise is shifted towards lower frequencies if inflow turbulence is present, along with an increased peak noise level. Issues for further research activities are pointed out.

1. Introduction

There is a wide consensus that turbulent boundary layer trailing edge noise (TBL-TEN) is the dominant source of aeroacoustic broadband noise emission of wind turbines (Oerlemans, Sijtsma, & Méndez López, 2007). TBL-TEN is also known as airfoil self-noise, since it is supposed not to be dependent on disturbances of the global flow field, provided that transition location is fixed. Wind turbines are operated in the turbulent atmospheric boundary layer containing turbulence length scales ranging from meso- to micro-scale. Turbulent inflow impinging the leading edge of an airfoil causes emission of turbulent inflow noise (Wagner, Bareiß, & Guidati, 1996). There is a wide basis of experimental, numerical and analytical work on TBL-TEN with steady inflow conditions. The data basis on noise emission with turbulent inflow conditions is considerably smaller, although wind energy applications take place under turbulent conditions. There are many reasons, ranging from difficulties in creating reproducible turbulence conditions to high computational costs due to the range of time scales to be covered in numerical simulations.

Amiet's model (Amiet, 1975) requires turbulence intensity and integral length scale as input parameters. However, in an atmospheric boundary layer most turbulent kinetic energy is contained in huge eddies which cause unsteady loads on aerodynamic surfaces but do not contribute to noise emission in the audible frequency range. These huge eddies also dominate the turbulence integral length scale. In Fig. 1, the different effects of large and small eddies on global and local blade loading are visualized. The properties of turbulence in the relevant range of length scales, say in the order of magnitude of the blade chord and smaller are described by model spectra depending on the largest eddies. No wonder that prescribing measured integral length scales and overall turbulence intensities yields wrong turbulent inflow noise emission results, if the model spectrum does not reproduce the relevant range of length scales correctly. Modifying the shape of the model spectrum seems more beneficial than fitting the integral

parameters so that predicted noise emissions match measured data. Unfortunately there is little reliable experimental data available for the relevant range of length scales including effects of complex terrain and weather conditions. Strong impact of thermal convection was shown by means of in-flight measurements by (Herrig & Würz, 2008). Further investigations in this field are desirable. Numerical simulations of the atmospheric boundary layer are restricted to large length scales due to computational cost limitations.

Another drawback of Amiet's model is that it does not account for airfoil geometry since it was deduced for a flat plate. Moriarty et al. introduced an empirical relation accounting for the airfoil thickness (Moriarty, Guidati, & Migliore, 2005). Moreover, Amiet's model deploys Taylor's hypothesis of frozen turbulence. Far away from the blade surface this seems appropriate, particularly when considering that the advection velocity of atmospheric turbulence is low compared to the velocity in the moving frame of reference of the rotor. However, strong velocity gradients in the vicinity of the leading edge question the validity of Taylor's hypothesis in this case.

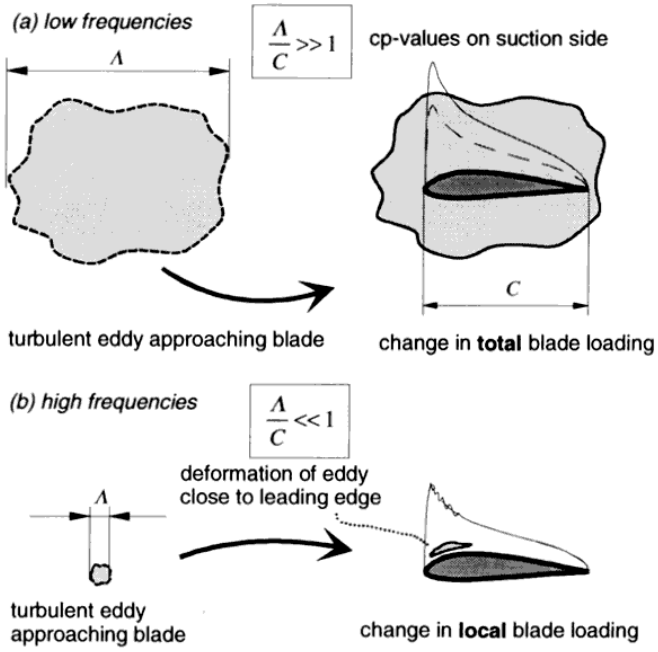

Fig. 1: Effect of small and large eddies approaching a blade (Wagner, Bareiß, & Guidati, 1996)

The research project "INFLOW-Noise" was originated to get more insight into the physics of the aforementioned aspects by means of numerical simulations and wind tunnel measurements of an airfoil in turbulent inflow. The scope of the present paper is to present first results of the numerical simulations of a generic test case corresponding to the wind tunnel set up. The airfoil was specifically designed for the wind tunnel measurements with the goal to generate high levels of both turbulent inflow noise and TBL-TEN in order to achieve noise levels significantly above the background noise of the wind tunnel. A detailed description of the airfoil design objectives and realisation can be found in (Illg, Neunaber, Lutz, & Krämer, 2015). The wind tunnel model is equipped with static and dynamic pressure transducers (Neunaber, Schultz-von Glahn, Illg, Peinke, & Hölling, 2015). All results presented in this paper were obtained at the design angle of attack of five degrees with attached turbulent boundary layer, avoiding undesired effects of separation noise. The operating Reynolds number is roughly one million. A first measurement campaign took place in 2014. Comparisons of experimental and numerical results will be subject of upcoming publications.

Recent results presented in this paper suggest that separating noise sources into an inflow turbulence depending part emitted at the leading edge and a part independent from inflow turbulence emitted at the trailing edge might not cover all effects due to inflow turbulence.

2. Numerical Methods and Setup

2.1 Flow Simulation

The CFD simulations are performed with the compressible finite-volume solver FLOWer, originally developed by the German Aerospace Centre (DLR) (DLR, 2006), (Kroll, Rossow, Schwamborn, Becker, & Heller, 2002) and continuously improved by the Institute of Aerodynamics and Gas Dynamics of the University of Stuttgart (IAG). Using a fifth order WENO (Weighted Essentially Non-Oscillatory) scheme for reconstruction of the convective flux together with a HLLC Riemann solver (Kowarsch, Keßler, & Krämer, 2013), (Kowarsch, Lippert, Schneider, Keßler, & Krämer, 2015) on block-structured grids together with the convergence

acceleration methods multigrid and dual time stepping, FLOWer is an efficient state of the art tool for high fidelity flow simulation, including Aeroacoustics. Flux conservative hanging grid nodes are implemented saving computational costs by means of a reduced overall grid cell number. For meshing complex geometries, the overset mesh method is used to overcome the drawbacks of structured grids. Several hybrid RANS/LES methods are implemented. Improved Delayed Detached Eddy simulation (IDDES) (Shur, Spalart, Strelets, & Travin, 2008) with Menter SST k-ω turbulence model (Menter, 1994) was used for the simulation of turbulent inflow noise presented in this paper. Grid induced separation, which is likely to occur at high levels of inflow turbulence is avoided, yet the RANS mode is restricted to a thin layer near the wall allowing the resolution of large vortices inside the outer boundary layer. The grid resolution is $x^+=100$, $y^+<=1$ and $z^+=200$ in the boundary layer and 1.1% of the chord in the inflow turbulence advection zone. In this region, as well as in the boundary layer, the fifth order WENO scheme is used, whereas in the remaining domains the second order JST scheme (Jameson, Schmidt, & Turkel, 1981) is used on a gradually coarsened mesh using hanging grid nodes towards the farfield boundaries. This reduces computational costs and provides faster dissipation of acoustic waves to avoid reflections at the boundary conditions. The airfoil boundary layer mesh is an overset mesh embedded in a Cartesian background mesh. All CFD simulations are performed on a Cray XC40 system at the High Performance Computing Centre Stuttgart (HLRS).

2.2 Inflow Turbulence and Simulation Domain

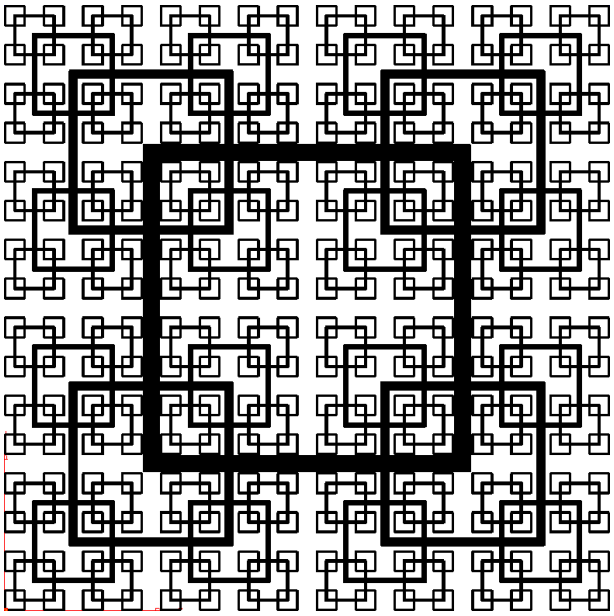

Fig. 2: Geometry of the fractal grid used for turbulence generation

The inflow turbulence is generated by a square fractal grid shown in Fig. 2 in the acoustic wind tunnel of the University of Oldenburg as well as in the simulation in order to achieve comparable inflow conditions. In the open jet of the wind tunnel the airfoil with a span of 0.8 m and a chord of 0.3 m is mounted between endplates. The simulation domain corresponds to the wind tunnel geometry. To allow the simulation of several angles of attack and different airfoils, turbulence generation and simulation of the airfoil in the turbulent flow are separated. The simulation of the turbulence in the wake of the fractal grid is performed by Fraunhofer IWES (Mihoubi, Rinn, & Stoevesandt, 2014). The turbulence downstream a fractal grid is mainly generated by interaction of the wakes of the individual grid elements, thus the wave numbers corresponding to the Strouhal numbers of the grid bars are superimposed by a broadband spectrum of turbulence length scales. Fractal grids generate higher turbulence intensities than regular grids with comparable blockage ratio (Mazellier & Vassilicos, 2010). The unsteady flow field obtained by the simulation of the wake of the fractal grid is injected into the airfoil simulation domain at a plane corresponding to the nozzle cross section of the open jet wind tunnel via a Dirichlet inflow boundary condition (Meister, Lutz, & Krämer, 2012). Fig. 3 gives an impression of the turbulent flow field around the airfoil. The mean flow velocities of simulation and experiment are matched using hot wire anemometry data.

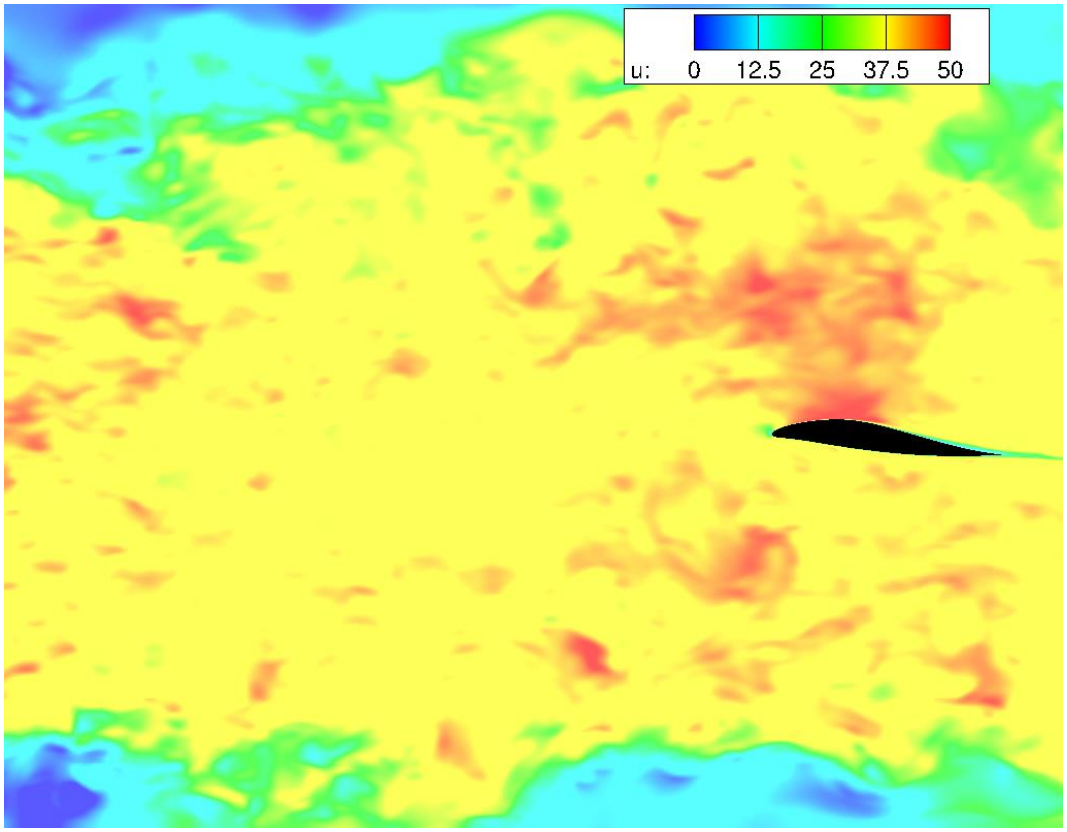

Fig. 3: Axial velocity contours u [m/s] illustrating the turbulent flow field around the airfoil

2.3 Trailing Edge Noise Prediction

The in-house code Rnoise (Kamruzzaman, 2012) is used to simulate TBL-TEN emissions based on an improved formulation of the TNO-Blake model (Parchen, 1998), including modelling of boundary layer turbulence anisotropy (Kamruzzaman, Lutz, Herrig, & Krämer, 2012). Noise prediction requires CFD simulation results applying various turbulence models, including RSM, of a turbulent boundary layer in the vicinity of the trailing edge as input. Results of an Rnoise analysis are local wall pressure fluctuations and the far field noise spectrum. Rnoise is thoroughly validated with wind tunnel measurements (Herr, Bahr, & Kamruzzaman, 2012). A detailed description of Rnoise and the improvements to the original TNO-Blake model can be found in (Lutz, et al., 2015).

Direct numerical simulation of the noise sources and the propagation of acoustic waves would be desirable since uncertainties of the applied model could be excluded. However, today's computational resources limit the application on low Reynolds numbers. For wind energy applications, modelling is inevitable.

The impact of inflow turbulence on TBL-TEN is examined by means of a decomposition of the fraction of the boundary layer turbulence resolved by the numerical scheme and the fraction modelled by the turbulence model as expressed by the following equation for the turbulence kinetic energy:

$$k_t = k_{t,resolved} + k_{t,modelled}$$

This approach allows the application of Rnoise for TBL-TEN prediction based on hybrid RANS/LES CFD simulations as well as on LES with a subgrid scale turbulence model. The results in this paper were obtained with time-averaged boundary layer data. Time-resolved application based on unsteady CFD simulations is also possible and will be performed in future.

2.4 Turbulent Inflow Noise Simulation

For the simulation of the propagation of turbulent inflow noise to the farfield, the in-house Ffowcs Williams-Hawkings (FW-H) (Williams & Hawkings, 1969) code ACCO (Keßler & Wagner, 2004) is used. The variables pressure, density and velocity of time-dependent CFD simulations are evaluated on predefined hull surfaces f_S yielding acoustic monopole and dipole sources. If the volume zone enclosed by the hull surface is also evaluated, quadrupole sources can be determined separately. The source terms constitute the right hand side of the FW-H equation, whereas the wave propagation equation is represented by the left hand side:

$$\frac{\bar{\partial}^2 \bar{\rho}'}{\partial t^2} - c^2 \bar{\nabla}^2 \bar{\rho}' = \frac{\partial^2}{\partial x_i \partial x_j}\left[T_{ij} H(f_s)\right] - \frac{\partial}{\partial x_i}\left[\left(p' n_i + \rho u_i (u_n - v_n)\right)\delta(f_s)\right] + \frac{\partial}{\partial t}\left[\rho_0 v_n + \rho(u_n - v_n)\right)\delta(f_s)\right]$$

All acoustic sources enclosed by those hull surfaces are included in the noise computation, whereas sources outside of the hull surfaces as well as hydrodynamic fluctuations do not contribute. This allows the separate observation of noise emitting zones like the leading edge, as well as the selection of zones with locally homogeneous inflow turbulence along the span. These options are the reason why the application of the FW-H solver is preferred over the direct computation of the propagation of acoustic waves (CAA approach). Furthermore, hydrodynamic pressure fluctuations do not contribute to the source terms of the FW-H equation, hence the selected approach is well suited for evaluating noise reception at observer positions within a turbulent flow field. Previous studies showed that the distance of the hull surface to the airfoil is not critical, even a hull surface directly on the airfoil surface yields good results. In this case, noise emitted by the turbulence itself is not included in the result, which is desirable if only noise emitted by the interaction of vortices with a rigid surface is of interest.

3. Noise Prediction Results

3.1 Turbulent Inflow Noise

For evaluation of the noise generated by inflow turbulence impinging the leading edge, the foremost 2.5 %, 20 % and 100 % of the chord were examined separately by means of corresponding hull surfaces at two spanwise segments with a span of 15 % chord. The two spanwise segments are located symmetrically to the centre line which allows averaging for accelerated statistical convergence and approximates locally homogeneous inflow turbulence. The observer position is located 1.0 m above the leading edge of the airfoil, normal to the mean flow direction. A scaling correction as proposed by (Kato, Idia, Tankano, Fujita, & Ikegawa, 1993) for a spanwise correlation length L_C smaller than the spanwise extent of the simulation domain L was applied to normalise the sound pressure level SPL with a span L_S of 1 m:

$$SPL = SPL + 10\log(L/L_S)$$

In Fig. 4**,** the resulting sound pressure level spectra and excerpts of the time series of pressure at the observer location are shown. All three spectra show broadband characteristics, however, they are not smooth. The reason for this can either be found in not sufficient statistical convergence or in dominant length scales present in the inflow turbulence. When a longer time series as a result of continued computation will be available, the former could be precluded. As to be expected, the amplitudes of the full chord evaluation envelop the amplitudes of the partial surface evaluations. A substantial percentage of noise is emitted within the foremost 20 % of the chord, whereas the share of the leading edge region in noise emission, within 2.5 % chord, is minor. This observation is a contradiction to Amiet's theory, where noise is emitted directly at the leading edge. However, Amiet's theory is based on a flat plate with a sharp-edged leading

edge representing a discontinuity. It is consequential that a finite leading edge radius spreads noise emission to a larger zone.

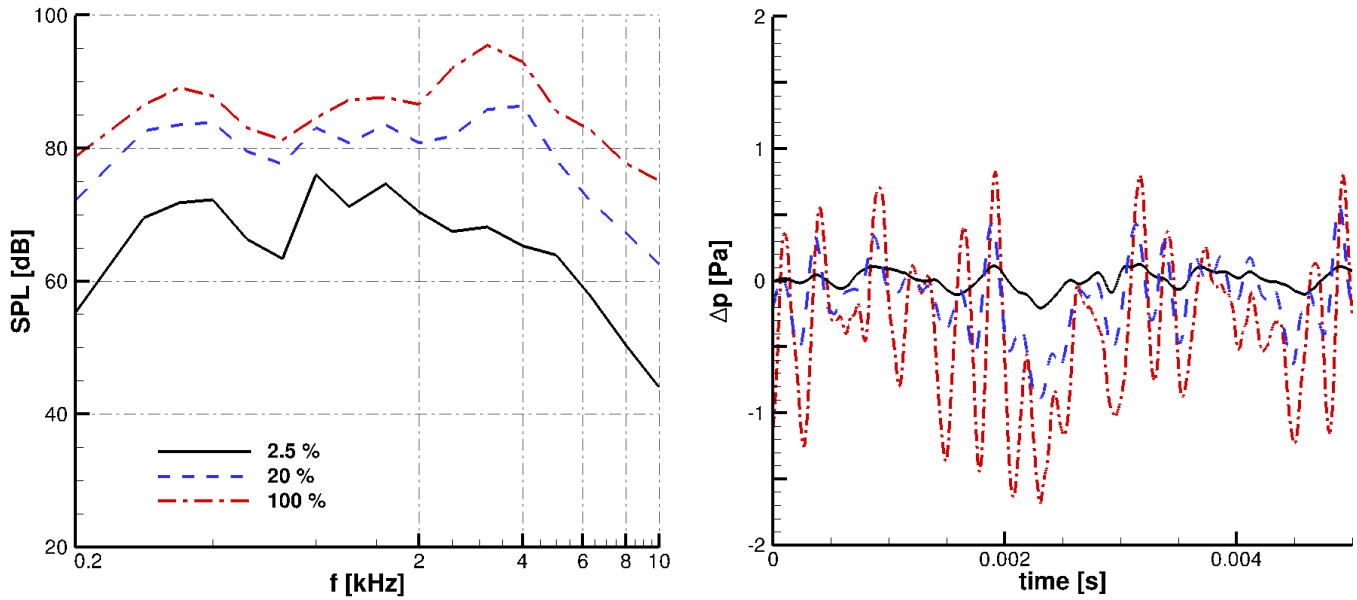

Fig. 4: Third octave spectra (left) and extracts of the time signals (right) of turbulent inflow noise emitted from the foremost 2.5 %, 20 % and the full chord of the airfoil

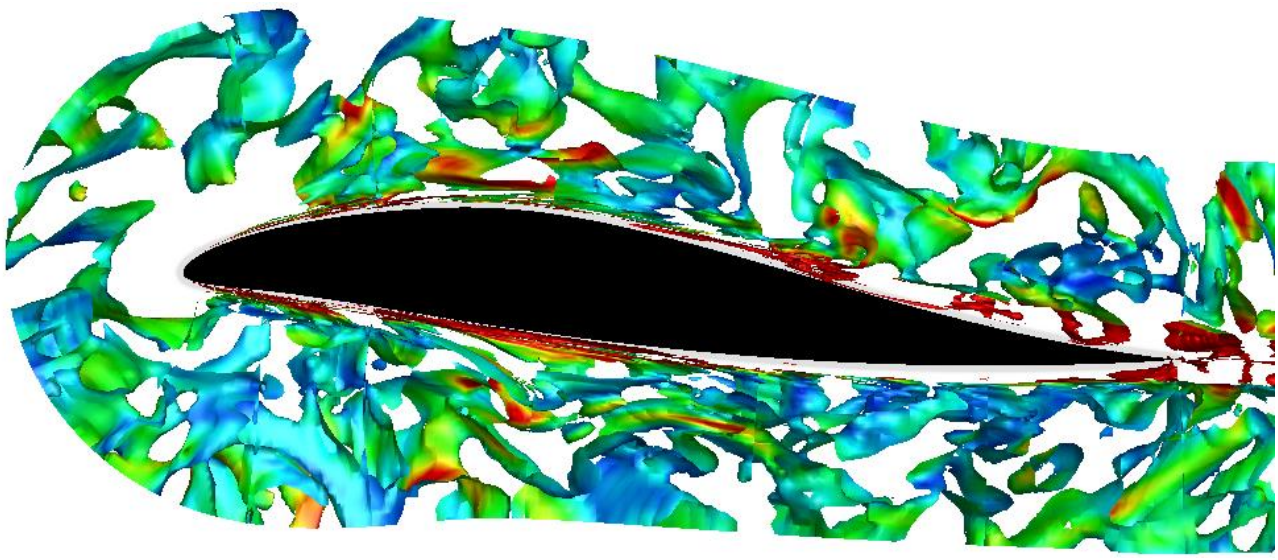

Fig. 5: Lambda-2 iso surfaces, colour indicates vorticity magnitude

Regarding the frequency distribution of the spectra, one notices that the peak frequency is lower at the leading edge, which suggests that vortices impinging the leading edge decay to smaller structures or existing smaller structures are amplified generating higher frequency noise emission on the airfoil surface downstream. To confirm this hypothesis, analysis of the development of spatial turbulence length scales around the airfoil will be performed in near future. As stretching of vortex lines plays a dominant role in decay to smaller structures, it is believed that this effect cannot be observed with harmonic waves parallel to the leading edge instead of three dimensional turbulence, which will be the concern of further studies. In any case, the presence of this effect confirms the relevance of the approach using turbulent inflow instead of the more straight forward approach using harmonic disturbances. An extract of the time signals of pressure fluctuation at the observer position was included in Fig. 4 to show the distinct correlation among pressure fluctuations stemming from different zones on the airfoil surface, which is most obvious among the 20 % and the full chord case. The time lag is caused by the advection velocity. The less pronounced correlation of the 2.5 % chord signal indicates

that turbulence properties are strongly modified in the leading edge region, most likely due to the prevailing high gradients of the flow field. Both effects, the generation of a large share of noise emission on the airfoil surface behind the leading edge and the modification of inflow turbulence parameters during the advection past the leading edge are evidence for the application of frozen turbulence hypothesis not to be physically correct. In Fig. 5, an increase in vorticity downstream the leading edge and the formation of smaller structures inside and outside the boundary layer is visible. Further studies will have to show if these observations have significant impact on noise prediction methods or if they are negligible.

3.2 Impact of Inflow Turbulence on Trailing Edge Noise

Trailing edge noise was computed by means of Rnoise (see section 2.3) for two cases, with and without inflow turbulence. For both cases, the mean inflow velocity is 40 m/s. The boundary layer was evaluated with Rnoise at 99.5 % chord on the suction side of the airfoil at the same span position where leading edge noise was evaluated (see previous paragraph). Transition is forced by means of a zig-zag tape at 5 % chord on pressure and suction side in the experiment. Fully turbulent flow was assumed for the simulation. In case of turbulent inflow, time-averaged values of the boundary layer data are used. The fraction of turbulence kinetic energy resolved by the numerical scheme is added to the fraction modelled by the turbulence model. For comparison, results considering only the modelled fraction are also included. The noise spectra, calculated for a span of 1 m and an observer position 1 m above the trailing edge, are shown in Fig. 6.

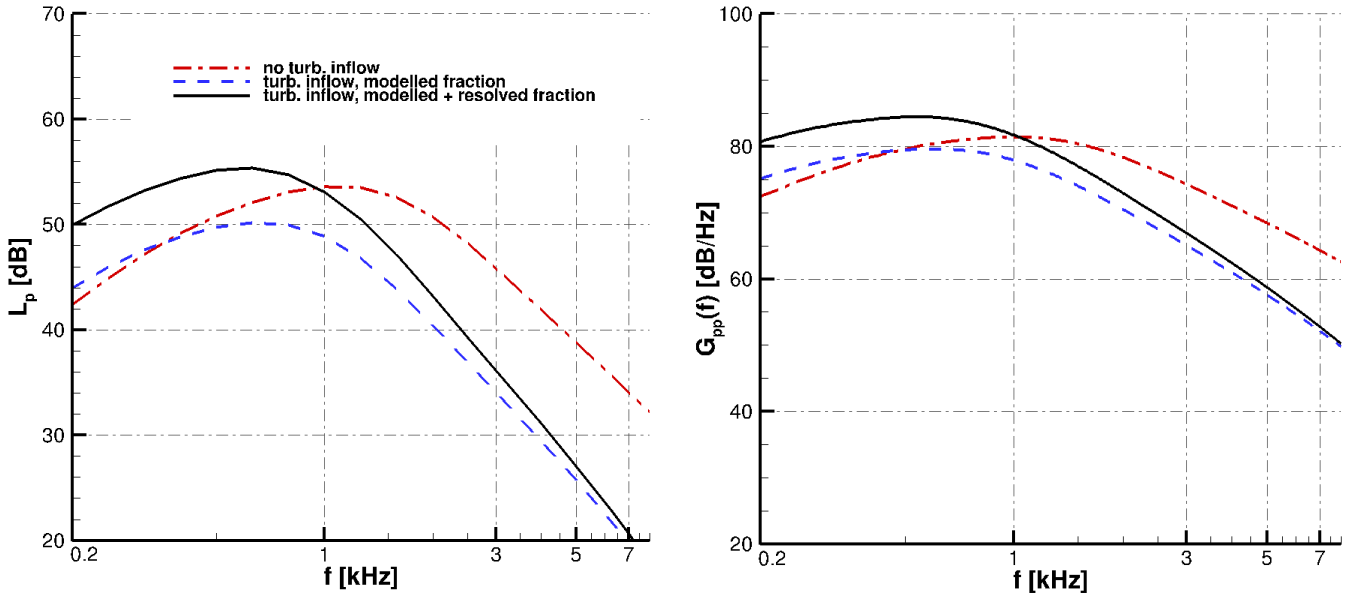

Fig. 6: Comparison of 1/3 octave sound pressure spectra (left) and narrow band spectra of the wall pressure fluctuations (right) with and without inflow turbulence

The peak frequency is considerably lower with turbulent inflow, since the boundary layer thickness almost doubles. When the resolved fraction of the turbulence is considered, the peak level is increased by 2 dB. As to be expected, the curves with and without resolved turbulence converge at high frequencies, since this part of the spectrum is dominated by small scales near the wall which are completely modelled. Large structures, especially outside the RANS layer near the wall, are resolved by the numerical scheme, hence the resolved fraction has a large impact on noise emission at low frequencies. Without the resolved fraction of the turbulence, the noise level is below the case without turbulent inflow. The explanation is that the turbulent inflow causes the thickness of the RANS layer determined by the IDDES approach to decrease leading to a decreased amount of modelled turbulence. The same qualitative relations can be seen in the wall pressure fluctuations at the trailing edge. I should like to point out that the

reduced peak frequency due to inflow turbulence is likely to mitigate the effect of increased unweighted sound pressure level due to reduced human reception at lower frequencies.
The authors are aware of the fact that LES simulations, as well as hybrid RANS/LES simulations are highly dependent of the grid resolution and the numerical method used. The results seem plausible, though careful validation is required. The experimental data obtained during the project will be useful. Further numerical studies with a refined boundary layer mesh allowing wall-modelled LES simulation are planned to get more insight into the interdependency of free stream turbulence and boundary layer turbulence.
These results advise to pay attention to the impact of inflow turbulence on TBL-TEN. However, the presented generic case precludes drawing direct conclusions on the impact on the noise emission of a rotor in turbulent conditions. Further numerical studies with commonly used airfoils and realistic turbulence intensities will be performed to overcome that issue.

4. Conclusions

The results presented in this paper show effects of three-dimensional inflow turbulence interacting with an airfoil and with a turbulent boundary layer. Some of the effects, namely the impact of strong velocity gradients near the leading edge on turbulence decay and interaction of free-stream turbulence with boundary layer turbulence cannot be observed with two-dimensional harmonic gusts impinging an airfoil. Therefore the sophisticated approach simulating a fully turbulent flow field is appropriate.
Due to the generic airfoil and generic inflow turbulence, the results cannot be directly transferred to wind energy applications. However, they provide a basis for further investigations and improve the comprehension of fundamental noise generation mechanisms beyond the scope of simplifying models. Simulations of rotor blade airfoils in realistic turbulent atmospheric inflow conditions are planned. The modification of inflow turbulence properties caused by the presence of an airfoil and the consequences on noise emission will be a future research subject.
One drawback of Amiet's turbulent inflow noise prediction model, the dependency on accurate characterisation of turbulence in the relevant wave number range in the atmospheric boundary layer, cannot be eliminated by detailed examination of the noise production mechanisms. However, an improvement of existing prediction models concerning influence of airfoil geometry and angle of attack is conceivable.
To the knowledge of the authors, there was little attention paid to the impact of inflow turbulence on trailing edge noise in the past. The presented results might draw interest in this topic.

References

Amiet, R. K. (1975). Acoustic radiation from an airfoil in a turbulent stream. *Journal of Sound and Vibration*, pp. 407-420.

DLR. (2006). *FLOWer Installation and User Manual. Version 2009.1.*

Herr, M., Bahr, C., & Kamruzzaman, M. (2012). Workshop Category 1: Trailing-Edge Noise. *Second Workshop on Benchmark Problems for Airframe Noise Computations (BANC-II).* Colorado Springs.

Herrig, A., & Würz, W. (2008). Untersuchungen zur atmosphärischen Turbulenz in Bodennähe. *Symposium für Segelflugzeugentwicklung*. Wasserkuppe, Germany.

Illg, J., Neunaber, I., Lutz, T., & Krämer, E. (2015). Numerische Untersuchung von Vorder- und Hinterkantenlärm eines Profils in turbulenter Anströmung. *Accepted for DAGA 2015 - 41. Jahrestagung für Akustik.* Nürnberg, Germany.

Jameson, A., Schmidt, W., & Turkel, E. (1981). Numerical Simulation of the Euler Equations by Finite Volume Methods Using Runge-Kutta Time Stepping Schemes. *AIAA journal*.

Kamruzzaman, M. (2012). *Study of turbulence anisotropy and its impact on flow induced noise emission.* Faculty of Aerospace Engineering and Geodesy, University of Stuttgart: Doctoral thesis.

Kamruzzaman, M., Lutz, T., Herrig, A., & Krämer, E. (2012). Semi-Empirical Modeling of Turbulent Anisotropy for Airfoil Self-Noise Predictions. *AIAA journal, 50*(1), pp. 46-6.

Kato, C., Idia, A., Tankano, Y., Fujita, H., & Ikegawa, M. (1993). Numerical prediction of aerodynamic noise radiated from low mach turbulent wake. *31st Aerospace Sciences Meeting and Exhibit.* Reno, NV: AIAA.

Keßler, M., & Wagner, S. (2004). Source-time dominant aeroacoustics. *Computers & fluids*(33), pp. 791-800.

Kowarsch, U., Keßler, M., & Krämer, E. (2013). High Order CFD-Simulation of the Rotor-Fuselage Interaction. *39th European Rotorcraft Forum.* Moscow.

Kowarsch, U., Lippert, D., Schneider, S., Keßler, M., & Krämer, E. (2015). Aeroacoustic Simulation of an EC145T2 Rotor in descent flight. *accepted for the 53th American Helicopter Society Annual Forum.* Virginia Beach, VA.

Kroll, N., Rossow, C. C., Schwamborn, D., Becker, K., & Heller, G. (2002). MEGAFLOW—a numerical flow simulation tool for transport aircraft design. *Proceedings ICAS Congress.*

Lutz, T., Arnold, B., Bekiropoulos, D., Illg, J., Krämer, E., Wolf, A., . . . Kamruzzaman, M. (2015). Prediction of Flow-Induced Noise Sources of Wind Turbines. In *accepted for Special Issue of the International Journal of Aeroacoustics.*

Mazellier, N., & Vassilicos, C. (2010). Turbulence without Richardson-Kolmogorov cascade. *Phys. Fluids, 22*.

Meister, K., Lutz, T., & Krämer, E. (2012). Time-Resolved CFD Simulation of a Turbulent Atmospheric Boundary Layer Interacting with a Wind Turbine. *Euromech Colloquium.* Oldenburg, Germany.

Menter, F. R. (1994). Two-equation eddy-viscosity turbulence models for engineering applications. *AIAA journal, 32*, S. 1598–1605.

Mihoubi, M., Rinn, P., & Stoevesandt, B. (2014). Higher-order statistical analysis of DDES simulation. *iTi 2014 - Conference on Turbulence.* Bertinoro, Italy.

Moriarty, P., Guidati, G., & Migliore, P. (2005). Prediction of turbulent inflow and trailing-edge noise for wind turbines. *11th AIAA/CEAS Aeroacoustics Conference.* Monterey, CA.

Neunaber, I., Schultz-von Glahn, M., Illg, J., Peinke, J., & Hölling, M. (2015). Experimentelle Untersuchung des Vorder- und Hinterkantenlärms eines Profils in turbulenter Strömung. *Accepted for DAGA 2015 - 41. Jahrestagung für Akustik.* Nürnberg, Germany.

Oerlemans, S., Sijtsma, P., & Méndez López, B. (2007). Location and quantification of noise sources on a wind turbine. *Journal of Sound and Vibration, 299*(4), pp. 869-883.

Parchen, R. (1998). *Report DRAW, a prediction scheme for trailing-edge noise based on detailed boundary-layer characteristics.* TNO Institute of Applied Physics.

Shur, M., Spalart, P., Strelets, M., & Travin, A. (2008). hybrid RANS-LES model with delayed DES and wall-modeled LES capabilities. *Int. J. Heat Fluid Flow, 29*, pp. 1638-1649.

Wagner, S., Bareiß, R., & Guidati, G. (1996). *Wind turbine noise.* Springer Berlin, Heidelberg.

Williams, J., & Hawkings, D. (1969). Sound generation by turbulence and surfaces in arbitrary motion. *Philosophical Transactions of the Royal Society of London. Series A, Mathematical and Physical Sciences*, pp. 321-342.

Acknowledgements

The results discussed in this paper were obtained in the ongoing project “INFLOW-Noise” funded by the German Federal Ministry for Economic Affairs and Energy. The authors gratefully acknowledge this contribution. The authors also acknowledge DLR (German Aerospace Centre) for providing the CFD code FLOWer and HLRS (High Performance Computing Centre Stuttgart) for providing the computational resources.